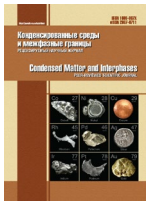

ISSN 1606-867X (Print)
ISSN 2687-0711 (Online)
Condensed Matter and Interphases
Kondensirovannye Sredy i Mezhfaznye Granitsy
https://journals.vsu.ru/kcmf/

Original articles

Research article
https://doi.org/10.17308/kcmf.2022.24/9860

Analysis of the variations in the surface properties of SiO_2 and Al_2O_3 nanoparticles obtained by different synthesis methods

V. V. Syzrantsev✉

Grozny State Oil Technical University,
100 Isaeva av., Grozny 364051, Russian Federation

Abstract

The article presents a comparative study of the surface properties of silica and alumina nanoparticles synthesized by various methods.

Using the IR spectroscopy we demonstrated that the synthesis method affect the surface properties of nanoparticles while maintaining the phase composition of the material. The article demonstrates the relationship between the types of surface sites, their strength, and the interaction of nanoparticles with the dispersed medium. In particular, a significant difference was observed in the strength of the active sites for all samples, which was reflected in the rheology of nanofluids based on epoxy resin. This demonstrates the importance of accurate descriptions of the surface properties of nanoparticles, as they determine their interaction with other materials.

The article also considers the possibility to evaluate the intensity of the particle-medium interaction based on the fractal dimension. Our study showed that it varies significantly depending on the synthesis method. The article discussed the possibility to determine the intensity of the particle-medium interaction using the values of the nanoparticle's zeta potential and the interfacial layer.

Keywords: Keywords: Nanoparticles, Surface sites, Interfacial layer, Zeta potential, Nanoparticle synthesis

Acknowledgements: The author expresses his gratitude to Professor E. I. Paukshist, DSc in Chemistry (G. K. Boreskov Catalysis Institute of the Siberian Branch of the Russian Academy of Sciences), and K. V. Zobov, PhD in Physics and Mathematics (Khristianovich Institute of Theoretical and Applied Mechanics of the Siberian Branch of the Russian Academy of Sciences), for the fruitful discussion of the results of the study.

For citation: Syzrantsev V. V. Analysis of the variations in the surface properties of SiO_2 and Al_2O_3 nanoparticles obtained by different synthesis methods. *Condensed Matter and Interphases*. 2022;24(3): 369–378. https://doi.org/10.17308/kcmf.2022.24/9860

Для цитирования: Сызранцев В. В. Контроль изменений свойств поверхности наночастиц SiO_2 и Al_2O_3, полученных разными методами. *Конденсированные среды и межфазные границы*. 2022;24(3): 369–378. https://doi.org/10.17308/kcmf.2022.24/9860

✉ Vyacheslav V. Syzrantsev, e-mail: vvveliga@mail.ru

1. Introduction

Nanoparticles are a common class of materials, whose properties have been studied in much detail. However, few researchers pay attention to the fact that, having the same chemical and phase compositions, some of the properties of nanoparticles depend on the conditions of their synthesis and may vary significantly [1]. At the moment, there are dozens, and for some substances even hundreds, of approaches to the synthesis of nanoparticles. The synthesis is always performed under certain conditions resulting in the formation of particles with specific crystal and surface structures. Therefore, powders synthesised using different methods are effective for different applications, and it is only possible to determine a suitable option for a particular application by trial and error. This appears to be the only reliable method, since there is no uniform approach to the characterisation of nanoparticles.

The significant difference between the characteristics of nanoparticles and bulk materials is quite often explained by the growing influence of the surface area, whose fraction in relation to the volume increases with the decrease in the size of the particles [2]. However, the changes in the properties of the surface itself, although crucial, are never taken into account. These changes may include surface defects (variations in the local coordination number, twinning, changes in the crystallographic planes, and porosity), the presence and composition of functional groups, and their inhomogeneity. These factors, except for lyophobic behaviour, are widely underestimated, even though they play an important role in the process of interaction of particles with a dispersed medium.

It is known that surface energy is proportional to the number of broken bonds in the surface atoms multiplied by the energy of these bonds. For particles with a metallic crystal structure this parameter helps to determine the melting point [3–5], as well as other thermodynamic parameters [6, 7] and the surface energy [8].

For oxides and more complex particles, the situation is more complicated.

Firstly, the existing descriptions of such nanoparticles, similar to bulk materials, mostly focus on their composition (purity) and size.

Secondly, such particles may be a combination of crystalline phases or be X-ray amorphous only in the order of short ranges [9, 10]. Since the surface energy can be different for different crystallographic planes on the surface of the particle [11], the identity of such particles can be questionable.

Thirdly, the surface of nanoparticles can have unique features which must be taken into account as opposed to the features of the surface of bulk materials. These features might include: porosity of the surface, the strength and concentration of Brønsted acid sites (BAS) and Lewis acid sites (LAS) [12], and ductility and elasticity of the neighbouring clusters comprising the particle.

For the gas-phase synthesis the key factors are the cooling rate and the mechanical and thermal properties of the cooling gas and the evaporated materials [13–16]. Additionally, the fast cooling rate of the vapour may result in a fixed metastable state of some of the clusters thus creating a ratio between the surface and the bulk energy characteristic for nanoparticles of a different size. In the case of a liquid-phase synthesis the result depends on the type of the process, the type of the reagent, the pH, the concentration of the precursor, the temperature, and the duration of the process [17]. The multicomponent sensitivity to the conditions of the synthesis results in significant variations of the size of the nanopaticles, their size distribution, and surface characteristics. Thus, during cryochemical condensation of silver vapour [18] different fractal dimensions of the particles were observed depending on the solvent: 1.9 (isopropanol), 1.7 (acetonitrile), 1.5 (toluene). The average sizes of the primary particles in the fractal cluster were 16.0, 21.0, and 9.4 nm respectively.

One of the most obvious methods to determine the difference in the interaction of nanoparticles of various origin with the medium they are dispersed in, is to measure its viscosity. The experimental studies [19, 20] demonstrated that higher concentrations and smaller size of the particles result in an increase in viscosity. However, the results obtained by different researchers vary greatly and are significantly higher than the values calculated using the the Batchelor–Green formula [21] commonly used for suspensions with microparticles. This can

be accounted for only by the variations in the interaction intensity between the liquid and nanoparticles [22] which differ in their surface structure, namely the thickness of the interfacial layer.

The variability of the surface properties occurring during the synthesis can be identified using IR and UV spectroscopy, which determine characteristic vibrations of bridging, terminal, and other bonds between the surface atoms. Thus, [1, 23] demonstrated that when different methods of synthesis of SiO_2 nanoparticles are used, their structure changes from close-packed (aerosils) to ribbon (silica gels). When the composition of the surface group is the same, the key factor is their inhomogeneity, i.e. their reactivity distribution. In particular, the ratio between the terminal and bridging OH groups may vary for nanoparticles [24]. A change in the number of Lewis acid sites can result from a number of factors including the changes in the local coordination number of oxygen, aluminium, silicon, or other elements of the oxide [25], thus reflecting the value of the surface energy of a particular sample.

Another way to determine the concentration of the active sites is by means of adsorption of acid-base indicators [[26]. Analysis of the adsorption spectra distribution makes it possible to predict the sorption capacity of the surface and other properties of nanoscale materials. In particular, it helps to determine the variations in the strength and concentration of BAS and LAS during the treatment of the surface and show their relation to the properties of the material, such as dielectric permittivity [27] and the coefficient of friction of the surface [28].

However, it is difficult to use the results of the IR spectroscopy and the indicator method directly due to their complexity and lack of transparency. Besides, the theoretical and practical aspects of the process need to be further elaborated by both researchers and manufacturers. Therefore, in our study, we analysed the results of the spectroscopy, particle-particle interaction based on the fractal dimension, and particle-medium interaction based on the viscosity measurements [29]. A fractal dimension is assumed to be a common factor which demonstrates the specifics of the interaction between particles and their environment or a material.

2. Materials and methods

To compare SiO_2 and Al_2O_3 nanoparticles we used samples obtained by several synthesis methods: SiO_2 and Al_2O_3 obtained by means of electron beam evaporation (Ts and Ta samples); commercially available SiO_2 and Al_2O_3 powders synthesised by pyrogenic process (As and Aa samples), (Evonik Industries, Germany); commercially available SiO_2 and Al_2O_3 powders obtained by liquid phase method (Ls and La samples), (Nanjing XFNANO Materials Tech Co., China); commercially available SiO_2 powders obtained using the plasma arc method (Psp sample), (Plasmotherm, Russia); commercially available Al_2O_3 AKP50 powders synthesised by means of chemical deposition (Sa sample) (Sumitomo Chemical, Japan); and commercially available Al_2O_3 powders obtained using the exploding wire method (Ea sample), (Perspektivnye Materialy, Russia). Their TEM photographs and particle size distribution are presented in Fig. 1–3. All silica particles were X-ray amorphous. Analysis performed by the Rietveld method demonstrated that their structural parameters and binding energies were similar. Aa and Ta samples were a gamma phase of aluminium oxide, and La, Ea, and Sa samples were an alpha phase of aluminium oxide. All particles were of spherical shape and had a similar average diameter. However, the range of particle size distribution varies greatly, which means that the particles will behave differently when applied for practical purposes.

For the IR spectroscopy, tablets were formed with the ratio of the mass to the geometric area being 15–49 mg/cm^2. The tablets were put into a vacuum IR cuvette and were vacuumized for 1 hour at 10^{-3} Pa. Then, without contact with the atmosphere, the samples were put into a measuring chamber, which measured the spectra at temperatures of up to 77 K. The spectra were then recorded at room temperature and at 77–110 K. The spectra were recorded using a Shimadzu IRTracer-100 spectrometer in the range of 600–6000 cm^{-1} with a resolution of 4 cm^{-1}. The number of accumulated scans was 100 which ensured the signal-to-noise ratio of at least 75000. The adsorption was performed at 77 K in doses which ensured the pressures of 0.1, 0.4, 0.9, 1.4, and 10 Torr in the cuvette.

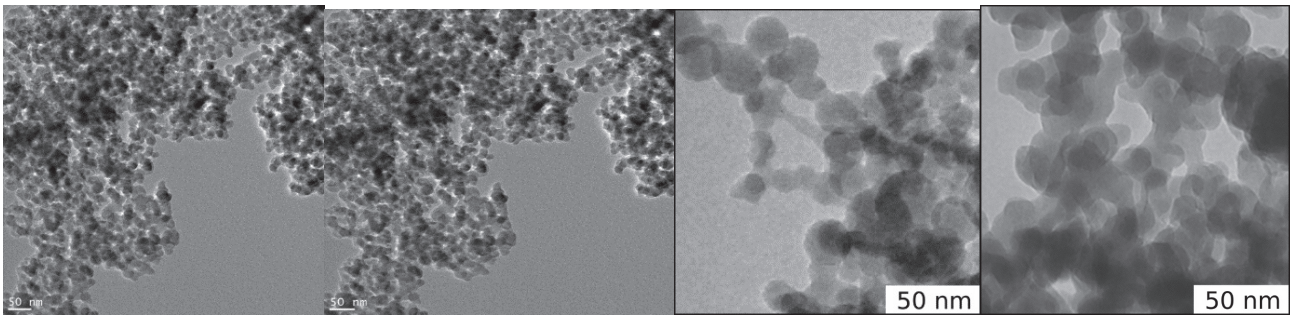

a b c d

Fig. 1. TEM photographs of SiO_2 nanoparticles: a) – sample Ls, b) – sample Ps, c) – sample Ts, d) – sample As

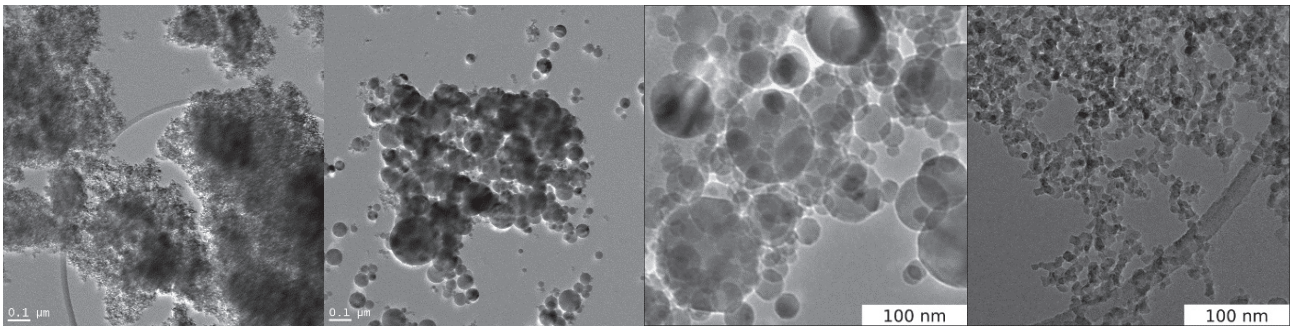

a b c d

Fig. 2. TEM photographs of Al_2O_3 nanoparticles: a) – sample La, b) – sample Ea, c) – sample Ta, d) – sample Aa

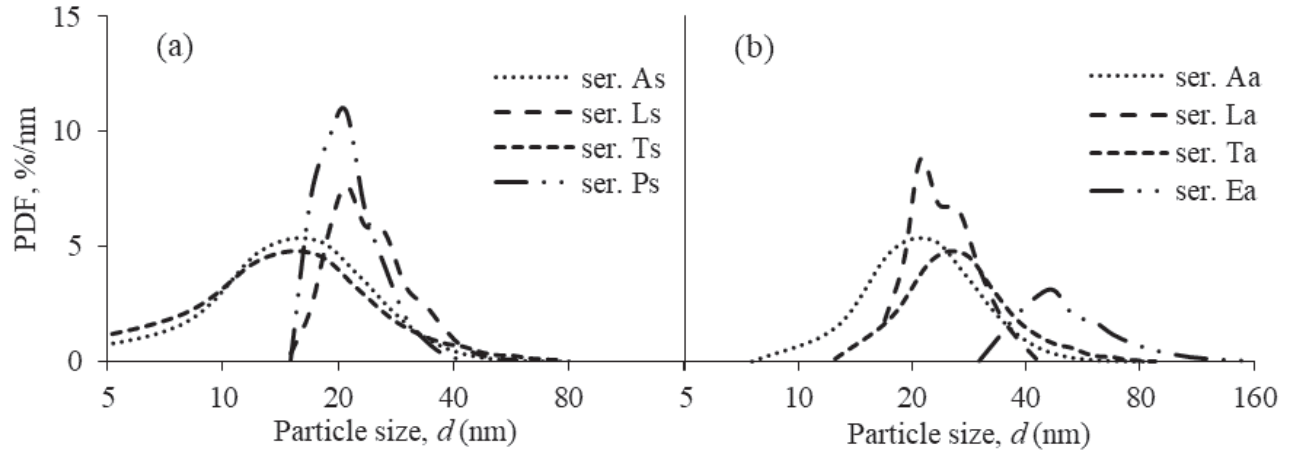

Fig. 3. Probability density function (PDF) of nanoparticle size distributions: (a) SiO_2; (b) Al_2O_3.

To measure the IR spectra of the adsorbed pyridine, the initial powders were mixed with barium fluoride at a ratio of 1:2. Barium fluoride was transparent in the region of 1000 cm^{-1} and thus did not distort the spectra in the region of OH groups. Prior to the adsorption of pyridine, the samples were vacuumized at 450 °C for 2 hours. The final pressure was below 10^{-3} Torr. Pyridine was adsorbed at a temperature of 150–160 °C for 15–20 minutes and then the air was evacuated for 60 minutes at the same temperature until the vacuum level was at least 10^{-2} Torr. The spectra were recorded with a resolution of 4 cm^{-1} in the region 1000–4000 cm^{-1} using a Shimadzu-8300 IR-Fourier spectrometer until 200 spectra were accumulated. The strength of the acid sites was qualitatively evaluated based on the position of two bands showing the vibrations of the pyridine ring in the regions 1440–1460 and 1590–1630 cm^{-1}.

The calculation methodology of the fractal dimension [30] is based on the linear dependence of the area of the agglomerate on its perimeter on double logarithmic scale. The calculation was performed based on the analysis of TEM photographs. Using photographs of various scales, for instance 50, 100, 200, and 500 nm, we obtained data on the similarity of particle agglomerations depending on the scale. Then from $\log S = C + 2/D \cdot \log P$ we obtained the fractal dimension D2 as the slope of the linear dependence of logS on logP. To obtain 3D fractal dimension D3 we recalculated the 2D values of D2 using the formula $D3 = 1.5 \cdot D2$. The measurement error was 0.005–0.01, which allowed us to use this parameter to assess the intensity of interaction between the particles and the medium.

3. Results

3.1. Variations in the fractal dimension

The fractal dimensions calculated for SiO_2 and Al_2O_3, nanoparticles are given in Fig. 4. As we can see, for all groups of SiO_2 nanoparticles fractal dimensions grow almost linearly with the growth of the specific surface in the range of 0.1–0.15. At the same time, the effect of the synthesis method can be stronger, reaching up to 0.4–0.5. The fractal dimension of Al_2O_3 nanoparticles (Fig. 4b) generally demonstrates a similar dependence. When the specific surface varies, the fractal dimensions of the particles of the same type are very close. When a different synthesis method is used, the difference is 0.3–0.5. The difference can also be accounted for by a different phase, since samples of Aa and Ta are gamma phase, and samples of La, Ea, and Sa are alpha phase. Nevertheless, the difference in the fractal dimension caused by the use of different synthesis methods is significant even for the same phase.

Summing up the data on all the types of particles, we can see that the particles synthesised using electron beam evaporation have smaller fractal dimension (2.3–2.6) than the particles synthesised by any other method. The largest fractal dimension, often close to the limit value ($D3_{max} = 3$), was observed in particles synthesised by liquid phase methods (Ls, La, Sa). Nanoparticles obtained by means of the pyrogenic process have intermediate values of fractal dimension whose range (2.3–2.7) varies significantly depending on the type of the synthesised material. Based on this data, we can assume that the fractal dimension reflects the difference in the force field of the surface of nanoparticles which forms agglomerates of various complex forms: sphere-like, ribbon, chain, jellyfish-like, etc. Under certain conditions it can be used as a basic identification parameter for the application of nanoparticles.

3.2. Variations in the surface properties

The most common surface defects are porosity and plane distortions (steps, depressions, twinning of the crystal lattice, and other distortions). In any case, the coordination numbers of the first and the last atoms change, affecting their ability to interact with the medium. This is how LAS appear,

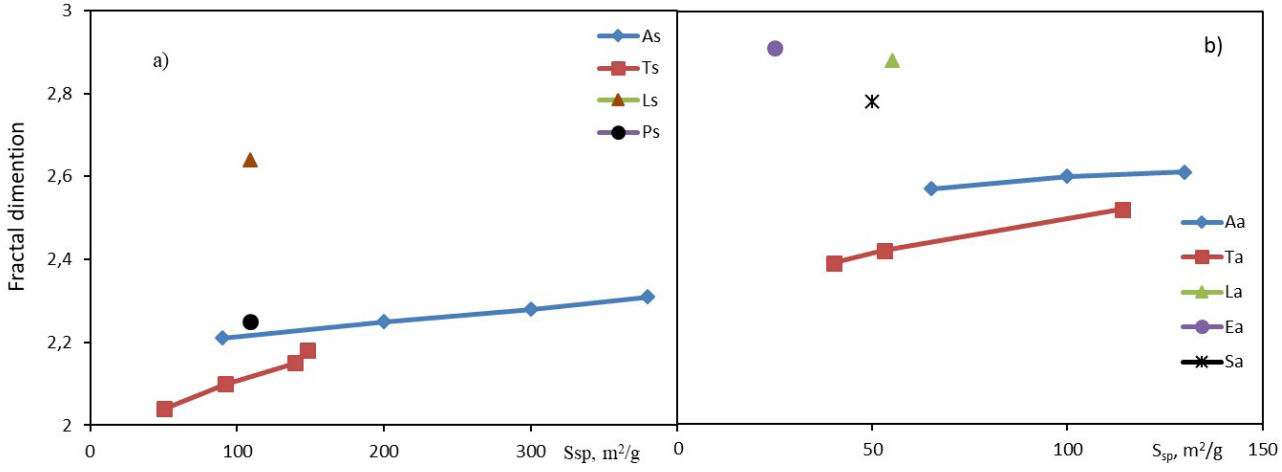

Fig. 4. The fractal dimension D3 of nanoparticles: a) – SiO_2 and b) – Al_2O_3

which result from coordinatively saturated metal cations in various coordination environment of, for instance, oxygen atoms (Fig. 5).

Another peculiar feature of the surface is the formation of OH groups, for instance terminal or bridge groups, which are easily identified in IR spectra based on the occurrence of absorption bands at 3400–3800 cm^{-1}. They are considered to be BAS. There can also be basic sites, i.e. bridge oxygen atoms or OH group oxygen atoms. Such surface properties are determined by means of IR spectroscopy, which can ensure the quite accurate identification of characteristic bands in the spectrum.

For SiO_2, the strength of the sites is determined based on the frequency shift of the OH stretching vibrations towards the region of low frequencies during the adsorption of CO. For Al_2O_3, the LAS strength is determined based on the shift of the bands of adsorbed pyridine at 1440–1460 cm^{-1} and 1590–1630 cm^{-1} to the region of high frequencies. The larger the shift, the stronger the asidic site. A number of studies of the said nanoparticles were carried out, and the difference in their structures was determined [10, 31, 32]. The results of the measurements are given in Table 1.

From the point of view of interactions with the medium, the strongest are the LAS which interact through the valence bonds of metals in the oxide. The next are basic sites interacting through oxygen atoms. The terminal OH groups, i.e. BAS are the weakest. Based on the analysis of the data on the SiO_2 samples, we can assume that the As sample demonstrates the highest intensity of the interaction with the medium due to the observed LAS (2200 cm^{-1}) and a significant shift of the frequency of stretching vibrations. The next is the Ps sample due to a significant shift in the frequency of stretching vibrations of the OH group (87 cm^{-1}) during the adsorption of CO. The third should be the Ts sample with a significant shift of the frequency of CO stretching vibrations (83 cm^{-1}). The Ls sample, with a shift of the frequency of stretching vibrations (79 cm^{-1}) and a strong BAS (2170 cm^{-1}), demonstrates the weakest interaction with the medium.

Similar conclusions can be made for the nanoparticles As and Ts obtained using the indicator method in [33]. The indicator method demonstrated that the surface of the As nanoparticles was mostly covered in LAS, while for the Ts sample, Lewis basic sites and BAS were observed.

As for the aluminium oxide, we can assume that the Aa sample (1454 and 1622 cm^{-1}) has the strongest interaction with the environment. The second is the Ta sample (1447 and 1604 cm^{-1}). At the same time, the La sample demonstrated medium LAS in the range of 2180–2197 cm^{-1}. The same for the Ea sample at 2189 cm^{-1}. They are thus compatible with regard to the intensity of their interaction with the medium.

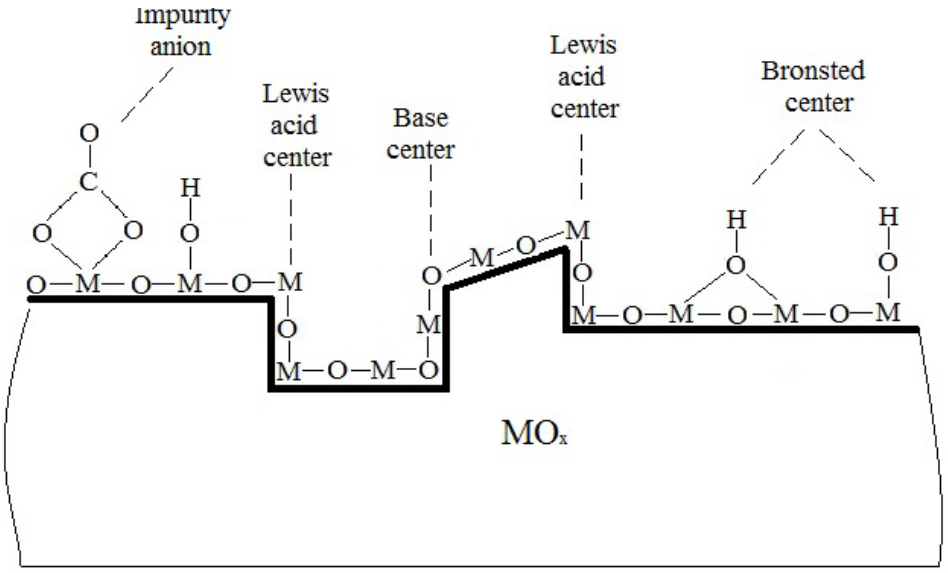

Fig. 5. Possible types of surface structures and sites

Table 1. Interpretation of the IR spectra (cm^{-1})

Sample SiO_2	Ls	Ps	Ts	As
Shift in the frequency of OH stretching vibrations of the SiOH groups	79	87	83	83
Medium LAS*	2170	none	none	none
Strong BAS*	none	none	none	2200
Hydrogen-bonded OH groups	none	weak 3650	3690, 3580	3690, 3580
Stressed Si-O-Si bridges	927	930	810	810
Stressed bridges	none	none	886, 946	886, 946
Sample Al_2O_3	La	Ea	Ta	Aa
Terminal OH groups (over 3750)	very weak 3795, 3780	very weak 3783	3785	strong 3785
Bridge OH groups (3650–3745)	weak 3680, 3695, 3732	3721, 3680 weaker than those of La	medium 3685, 3745, weak 3660	strong 3685, medium 3745, weak 3660
Medium LAS*	2180-2197	2189	none	none
Medium BAS**	2164	none	none	none
LAS** in the ranges of:				
1440–1460	none	none	1447	1454
1590–1630	none	none	1604	1622

* according to the stretching vibrations of the adsorbed CO
** according to the spectra of the adsorbed pyridine

3.3. Variations in the interaction intensity

Experimental measurements of the ζ-potential and the thickness of the interfacial layer [29] according to the model presented in [22] demonstrated that there is a strong correlation between these values, which indicates their affinity. From the point of view of colloidal chemistry, the ζ-potential is determined by the intensity of the interaction between the particle and the medium and corresponds to the thickness of the layer where the medium connected with the particle and divided from it is dispersed (Stern layer [34]). The result of the comparison (Table 2) demonstrates the presence of a linear dependence of the thickness of the interfacial layer δ, obtained based on the measurements of the viscosity of the nanofluid on the value of the ζ-potential. This means that the surface structure and the value of the ζ-potential connected with it, which determine the intensity of the interaction of the particles with the medium, depend more on the synthesis method rather than on the size of the particles.

Comparing the data from Table 2 and the assumptions regarding the interaction intensity based on the IR spectroscopy, we can see that they are almost identical. The thickness of the interfacial layer corresponding to the interaction intensity is the largest for the the As sample, and then deteriorates in the same order as determined by the IR spectroscopy. A slight difference can be accounted for by the possible affinity of the resin to the specific surface groups, or by some additional factors. Aluminium oxide samples demonstrated the same correlation. The only difference is the use of electroexplosive particles (Ea) in the epoxy resin, where their effect on the viscosity is significantly stronger than the expected value.

The fractal dimension is not so obviously connected with the interaction intensity. We assume that the most effective is the value of 2.3–2.5, while the almost ideal values ($D3_{max} = 3$) make the interaction with the medium less intensive. This is analogous to the process of cluster formation up to the point when a metastable isomer state is reached. It is known that at this point diffusion-limited aggregation of molecules is no longer a priority, because the system is ideal, and therefore it is more profitable to grow new clusters. In this case, the effective interaction between the particles and the environment

Table 2. Characteristics of SiO_2 and Al_2O_3 nanoparticles

Sample SiO_2	Ls	Ps	Ts	As
Fractal dimension	2.640±0.005	2.250±0.006	2.04-2.18±0.01	2.21-2.31±0.01
ζ-potential, mV	−21.2±0.5	−24.2±0.7	−30.2±0.6	−36.2±0.5
Thickness of the interfacial layer in ED-20, δ, nm	2.82	3.03	3.29	3.67
Sample Al_2O_3	La	Ea	Ta	Aa
Fractal dimension	2.880±0.005	2.910±0.005	2.39–2.52±0.01	2.57-2.61±0.01
ζ-potential, mV	13.3±0.5	−17.5±0.4	−7.8±0.3	−12.8±0.6
Thickness of the interfacial layer in ED-20, δ, nm	0.5	2.54	1.89	2.23

requires available LAS bonds, which form on the defects of the surface. At the same time, low D3 prevents the formation of stable bonds between the atoms of the nanoparticles and the medium, also resulting in an insignificant increase in viscosity.

Therefore, the conducted study of the connection between the properties of the nanoparticles and their interaction with the medium demonstrated that it is possible to identify the particles by certain available parameters. The study thus provides researchers with a tool for forecasting the technological processes in this very complicated segment of nanotechnologies.

4. Conclusions

The article discussed the necessity to take into account the synthesis method when designing the technological processes with nanoparticles, since it determines the effectiveness of interaction of the particles with the medium. We suggest that the composition of the surface particle sites, which determine the intensity of their interaction with the environment, should be taken into account, namely LAS, basic sites, and BAS. The article demonstrated examples of the effect of such sites for the silica and alumina nanoparticles synthesised by means of several methods. The correspondence with the surface properties is not uniform and it is necessary to take into account surface forces. Therefore, the quality control of the full-scale production requires the control over the stability of size distribution of the particles and the fractal dimensions.

Conflict of interests

The author declares that they have no known competing financial interests or personal relationships that could have appeared to influence the work reported in this paper.

References

1. Sheka E. F., Khavryuchenko V. D., Markichev I. V. Techonological polymorphism of disperse amorphous silicas: inelastic neutron scattering and computer modelling. *Russian Chemical Reviews*. 1995;64(5): 389–414. https://doi.org/10.1070/rc1995v-064n05abeh000156

2. Vollath D., Fischer F. D., Holec D. Surface energy of nanoparticles – influence of particle size and structure. *Beilstein Journal of Nanotechnology.* 2018;9: 2265–2276. https://doi.org/10.3762/bjnano.9.211

3. Cluskey P. D., Newport R. J., Benfield R. E., Gurman S. J., Schmidt G. Z. An EXAFS study of some gold and palladium cluster compounds. *Zeitschrift for Physik D Atoms, Molecules and Clusters.* 1993;26: 8–11. https://doi.org/10.1007/bf01425601

4. Eckert J., Holzer J. C., Ahn C. C., Fu Z., Johnson W. L. Structural and thermodynamic properties of nanocrystalline fcc metals prepared by mechanical attrition. *Nanostructured Materials*. 1993;2: 407–413. https://doi.org/10.1016/0965-9773(93)90183-c

5. Coombes C. J. The melting of small particles of lead and indium. *Journal of Physics F: Metal Physics.* 1972;2: 441–449. https://doi.org/10.1088/0305-4608/2/3/013

6. Shandiz A., Safaei M. A. Melting entropy and enthalpy of metallic nanoparticles. *Materials Letters*. 2008;62: 3954–3956. https://doi.org/10.1016/j.matlet.2008.05.018

7. Safaei A., Shandiz M. A. Size-dependent thermal stability and the smallest nanocrystal. *Physica E: Low-dimensional Systems and Nanostructures.* 2009;41: 359–364. https://doi.org/10.1016/j.physe.2008.07.023

8. Ouyang G., Tan X., Yang G. Thermodynamic model of the surface energy of nanocrystals. *Physical Review B.* 2006;74: 195408. https://doi.org/10.1103/physrevb.74.195408

9. Abzaev Y. A., Syzrantsev V. V., Bardakhanov S. P. Simulation of the structural state of amorphous phases in nanoscale SiO_2 synthesized via different methods.

Physics of the Solid State. 2017;59(9): 1874–1878. https://doi.org/10.1134/S1063783417090025

10. Syzrantsev V., Paukshtis E., Larina T., Chesalov Y., Bardakhanov S., Nomoev A. Features of surface structures of alumina and titanium dioxide nanoparticles produced using different synthesis methods. *Journal of Nanomaterials*. 2018;2018: 1-10. https://doi.org/10.1155/2018/2065687

11. Fried E., Gurtin M. E. A unified treatment of evolving interfaces accounting for small deformations and atomic transport with emphasis on grain-boundaries and epitaxy. In: *Advances in Applied Mechanics*. Aref H., van der Giessen E. (eds.). Academic Press: San Diego, CA, U.S.A.; 2004. pp. 1–177. https://doi.org/10.1016/s0065-2156(04)40001-5

12. Chukin G. D., Smirnov B. V., Malevich V. I. Formation of the structure of an amorphous aluminosilicate catalyst and its Lewis acid sites. *Kinetics and Catalysis*. 1988;29(3): 609-615.

13. Yumozhapova N. V., Nomoev A. V., Syzrantsev V. V., Khartaeva E. C. Formation of metal/semiconductor Cu-Si composite nanostructures. *Beilstein Journal of Nanotechnology*. 2019;10: 2497–2504. https://doi.org/10.3762/bjnano.10.240

14. Grammatikopoulos P., Steinhauer S., Vernieres J., Singh V., Sowwan M. Nanoparticle design by gas-phase synthesis. *Advances in Physics: X*. 2016;2: 1–20. https://doi.org/10.1080/23746149.2016.1142829

15. Swiatkowska-Warkocka Z., Koga K., Kawaguchi K., Wang H., Pyatenko A., Koshizaki N., Pulsed laser irradiation of colloidal nanoparticles: a new synthesis route for the production of non-equilibrium bimetallic alloy submicrometer spheres *RSC Adv*. 2013;3: 79–83. https://doi.org/10.1039/c2ra22119e

16. Li C., Yamauchi Y. Facile solution synthesis of Ag@Pt core-shell nanoparticles with dendritic Pt shells. *Physical Chemistry Chemical Physics*. 2013;15: 3490–3496. https://doi.org/10.1039/c3cp44313b

17. Kaabipour S., Hemmati S. A review on the green and sustainable synthesis of silver nanoparticles and one-dimensional silver nanostructures. *Beilstein Journal of Nanotechnology*. 2021;12: 102–136. https://doi.org/10.3762/bjnano.12.9

18. Kato M. Preparation of ultrafine particles of refractory oxides by gas-evaporation method. *Japanese Journal of Applied Physics*. 1976;15(5): 757–760. https://doi.org/10.1143/JJAP.15.757

19. Minakov A., Rudyak V. Ya, Pryazhnikov M. I. Systematic experimental study of the viscosity of nanofluids. *Heat Transfer Engineering*. 2021;42(12): 1024–1040. https://doi.org/10.1080/01457632.2020.1766250

20. Bashirnezhad K., Bazri S., Safaei M., Goodarzi M., Dahari M., Mahian O., Dalkılıça A., Wongwises S. Viscosity of nanofluids: a review of recent experimental studies. *International Communications in Heat and Mass Transfer*. 2016;73(4): 114–123. https://doi.org/10.1016/j.icheatmasstransfer.2016.02.005

21. Batchelor G. K. The effect of Brownian motion on the bulk stress in a suspension of spherical particles. *Journal of Fluid Mechanics*. 1977;83(1): 97-117. https://doi.org/10.1017/S0022112077001062

22. Syzrantsev V. V., Zavyalov A. P., Bardakhanov S. P. The role of associated liquid layer at nanoparticles and its influence on nanofluids viscosity. *International Journal of Heat and Mass Transfer*. 2014;72: 501. https://doi.org/10.1016/j.ijheatmasstransfer.2013.12.082

23. Khavryuchenko V. D., Sheka E. F. Computational modeling of amorphous silica. 4. Modeling the initial structures. Aerogel. *Journal of Structural Chemistry*. 1994;35(3): 305–308. https://doi.org/10.1007/BF02578281

24. Lamberov V. F., Romanova A. A., Shmelev R. G., Sopin I. G., Characterization of acid-modified alumina as a support for reforming catalysts. *Kinetics and Catalysis*. 2020;61(1): 130–136. https://doi.org/10.1134/s0023158420010097

25. Morterra G., Bolis C., Magnacca V. IR spectroscopic and microcalorimetric characterization of Lewis acid sites on (transition phase) Al_2O_3 using adsorbed CO. *Langmuir*. 1994;10(6): 1812–1824. https://doi.org/10.1021/la00018a033

26. Nechiporenko A. P. *Donor-acceptor properties of the surface of solid-phase systems. Indicator method*. St. Petersburg: Lan' Publ.; 2017. 284 p.

27. Sychev M. M., Cheremisina O. A. Relationship between the acid-base properties of the filler surface and the dielectric constant of polymer composite materials based on it. *ChemChemTech*. 2014;57(12): 67–71. (In Russ.). Available at: https://elibrary.ru/item.asp?id=23206884

28. Syrkov A. G., Silivanov M. O., Sychev M. M., Rozhkova N. N. Alteration of the acid-base properties of the oxidized surface of disperse aluminum during the adsorption of ammonium compounds and the antifriction effect. *Glass Physics and Chemistry*. 2018;44(5): 474–479. https://doi.org/10.1134/s1087659618050206

29. Syzrantsev V. V., Arymbaeva A. T., Zavjalov A. P., Zobov K. V. The nanofluids' viscosity prediction through particle-media interaction layer. *Materials Physics and Mechanics*. 2022; 48(3): 386-396. http://dx.doi.org/10.18149/MPM.4832022_9

30. Nomoev A. V., Vikulina L. S. Fractal dimension of the grain boundaries in ceramics with nanodispersed additions. *Technical Physics*. 2012;57(12): 1746–1748. https://doi.org/10.1134/s1063784212120225

31. Syzrantsev V. V., Larina T. V., Abzaev Yu. A., Paukstis E. A., Kostyukov A. I. Structural, surface and optical properties of nanoalumina produced by various

ways. *IOP Conference Series: Materials Science and Engineering*/ 2020;1000(1): 012001. https://doi.org/10.1088/1757-899x/1000/1/012001

32. Syzrantsev V. V., Paukstis E. A., Larina T. V. Surface polymorphism of silica nanoparticles. *IOP Conference Series: Materials Science and Engineering*. 2020;1008(1): 012030. https://doi.org/10.1088/1757-899x/1008/1/012030

33. Bardakhanov S. P., Vasiljeva I. V., Mjakin S. V., Kuksanov N. K. Surface functionality features of nanosized silica obtained by electron beam evaporation at ambient pressure. *Advances in Materials Science and Engineering*. 2010;2010: 241695. https://doi.org/10.1155/2010/241695

34. Mewis J., Wagner N. J. Colloidal suspension rheology. Cambridge University Press; 2011. https://doi.org/10.1017/CBO9780511977978

Information about the authors

Vyacheslav V. Syzrantsev, Cand. Sci. (Phys.–Math.), Director of the Research Centre for Collective Use of Scientific Equipment "Nanotechnologies and Nanomaterials", Grozny State Oil Technical University (Grozny, Russian Federation).

https://orcid.org/0000-0001-5388-8224

vvveliga@mail.ru

Received 20.03.2022; approved after reviewing 22.04.2022; accepted for publication 15.05.2022; published online 25.09.2022.

Translated by Yulia Dymant

Edited and proofread by Simon Cox